

Expression of SOD and APX genes positively regulates secondary cell wall biosynthesis and promotes plant growth and yield in *Arabidopsis* under salt stress

Amrina Shafi · Rohit Chauhan · Tejpal Gill · Mohit K. Swarnkar · Yelam Sreenivasulu · Sanjay Kumar · Neeraj Kumar · Ravi Shankar · Paramvir Singh Ahuja · Anil Kumar Singh

Received: 26 August 2014 / Accepted: 18 February 2015 / Published online: 10 March 2015
© Springer Science+Business Media Dordrecht 2015

Abstract Abiotic stresses cause accumulation of reactive oxygen species (ROS), such as hydrogen peroxide (H_2O_2) in plants. Sophisticated mechanisms are required to maintain optimum level of H_2O_2 that acts as signalling molecule regulating adaptive response to salt stress. CuZn-superoxide dismutase (CuZn-SOD) and ascorbate peroxidase (APX) constitute first line of defence against oxidative stress. In the present study, *PaSOD* and *RaAPX* genes from *Potentilla atrosanguinea* and *Rheum australe*, respectively were overexpressed individually as well as in combination in *Arabidopsis thaliana*. Interestingly, *PaSOD* and dual transgenic lines exhibit enhanced lignin deposition in their

vascular bundles with altered S:G ratio under salt stress. RNA-seq analysis revealed that expression of *PaSOD* gene in single and dual transgenics positively regulates expression of lignin biosynthesis genes and transcription factors (NACs, MYBs, C3Hs and WRKY), leading to enhanced and ectopic deposition of lignin in vascular tissues with larger xylem fibres and alters S:G ratio, as well. In addition, transgenic plants exhibit growth promotion, higher biomass production and increased yield under salt stress as compared to wild type plants. Our results suggest that in dual transgenics, ROS generated during salt stress gets converted into H_2O_2 by SOD and its optimum level was maintained by APX. This basal level of H_2O_2 acts as messenger for transcriptional activation of lignin biosynthesis in vascular tissue, which provides mechanical strength to plants. These findings reveal an important role of *PaSOD* and *RaAPX* in enhancing salt tolerance of transgenic *Arabidopsis* via increased accumulation of compatible solutes and by regulating lignin biosynthesis.

Electronic supplementary material The online version of this article (doi:10.1007/s11103-015-0301-6) contains supplementary material, which is available to authorized users.

A. Shafi · R. Chauhan · T. Gill · M. K. Swarnkar · Y. Sreenivasulu · S. Kumar · R. Shankar · P. S. Ahuja (✉) · A. K. Singh (✉)
Division of Biotechnology, CSIR-Institute of Himalayan Bioresource Technology, Palampur 176061, HP, India
e-mail: psahuja@ihbt.res.in

A. K. Singh
e-mail: anils13@gmail.com; anil@ihbt.res.in

A. Shafi · P. S. Ahuja · A. K. Singh
Academy of Scientific and Innovative Research, New Delhi, India

Present Address:
T. Gill

National Institute of Arthritis and Musculoskeletal and Skin Diseases, National Institute of Health, Bldg 10 CRC, 1-5256, 9000 Rockville Pike, Bethesda, MD 20892, USA

N. Kumar
Natural Plant Product Division, CSIR-Institute of Himalayan Bioresource Technology, Palampur 176061, HP, India

Keywords Ascorbate peroxidase · *Arabidopsis thaliana* · CuZn-superoxide dismutase · Hydrogen peroxide signalling · Lignification · RNA-seq · Secondary cell wall biosynthesis

Introduction

In living organisms, reactive oxygen species (ROS) are produced as a result of the stress conditions. ROS molecules include free radicals such as superoxide (O_2^-), hydroxyl radical ($\cdot OH$) and non radical molecules like hydrogen peroxide (H_2O_2) and singlet oxygen (1O_2). Superoxide dismutase (SOD) converts superoxide radical to H_2O_2 , while ascorbate peroxidase (APX) catalyses conversion of H_2O_2

to water and oxygen (Asada 1999). H_2O_2 at lower concentration participates in signalling pathways and cellular responses, such as the production of stress related proteins, upregulation of antioxidant molecules and enzymes and in the accumulation of compatible solutes (Vierling and Kimpel 1992; Miller et al. 2010). But at higher concentration, it oxidizes cellular components such as lipids, proteins and nucleic acids, cause inhibition of photosynthetic apparatus and can initiate chain reactions triggering cellular apoptosis (Zhu 2002).

Cell-wall lignification occurs as a stress response and provides structural rigidity and durability to plant tissues (Kim and Barbara 2008). Salinity stress has been associated with a higher deposition of lignin in vascular tissues and/or xylem development. In the central vascular cylinder of NaCl-treated wheat roots, the cell walls were found to be much thicker than those in control seedlings (Jbir et al. 2001). The increased number of lignified tracheary elements was observed in tomato roots under salinity stress, which enhances the cell-to-cell pathway for water transport and ion uptake (Sánchez-Aguayo et al. 2004). In soybean roots, salinity stress retarded primary xylem differentiation, but induced the development of secondary xylem (Hilal et al. 1998). In addition, Karahara et al. (2004) reported that the width of the lignified region of Casparian strip was increased under salinity stress in maize roots. Production of H_2O_2 in the lignified xylem elements has been presumed to be a strong trigger of initiation of the peroxidase-dependent oxidation of cinnamyl alcohol to lignins (Almagro et al. 2009). Low levels of H_2O_2 help in cell wall polymerization and generation of secondary messengers for signal transduction pathways (Neill et al. 2002). A primary oxidative activity which occurs during the lignification of lupin hypocotyls was reported to be carried out by H_2O_2 -dependent peroxidases (Ros-Barceló 1995). Several histochemical and biochemical studies have reported the presence of endogenous H_2O_2 in lignifying cells (Olson and Varner 1993). Higher plants respond to stress conditions by modifying the cell wall composition through changes in the activity of enzymes required for its formation. For example, expression pattern of a peroxidase in tomato (TPX1), which is involved in the synthesis of lignin, increased in response to salinity stress (Quiroga et al. 2000).

Localization of “cytosolic” CuZn-SOD near the vacuole and the apoplastic region, where superoxide molecules are generated was shown to be involved in the lignification process (Ogawa et al. 1996). Later, NAD(P)H oxidase was shown to provide superoxide anions as substrates to CuZn-SOD for production of H_2O_2 that helps the cell wall lignification (Ogawa et al. 1997). The involvement of SOD and H_2O_2 in cell wall lignification was further supported by several groups independently (Karpinska et al. 2001; Kim and Barbara 2008). However, the signal transduction

pathway of cell wall lignifications that uses H_2O_2 as signalling molecule under salt stress is not fully understood.

High altitude ecosystems are often inhabited by a very few plant species due to prevailing harsh environmental conditions. The genes/proteins isolated from high altitude plants are being used as molecular tools for engineering crop and other plants for better stress tolerance and adaptability against the present scenarios of climate change. In this pursuit, previously we identified and characterized a thermo-tolerant copper–zinc superoxide dismutase from a high altitude plant *Potentilla atrosanguinea* (*PaSOD*), which retains its activity even after autoclaving and also in the presence of NaCl (Kumar et al. 2002). In the present study, we have developed three types of transgenics in *Arabidopsis*, (a) overexpressing *PaSOD* gene, which converts superoxide anions into H_2O_2 , (b) overexpressing ascorbate peroxidase gene, *RaAPX* from another high altitude plant *Rheum australe*, which converts H_2O_2 molecules into water and (c) overexpressing both, *PaSOD* and *RaAPX* where H_2O_2 generated by *PaSOD* is metabolized by *RaAPX*. The detailed analysis revealed that these transgenics exhibit improved salt tolerance as compared to wild type (WT). Further analysis showed that transgenics had higher lignification of xylem and interfascicular cambium than WT mainly due to upregulation of genes involved in secondary cell wall biosynthesis. Our study suggests that the optimum levels of extracellular H_2O_2 regulated by antioxidant enzymes CuZn-SOD and APX, affect the secondary cell wall biosynthesis during salt stress which provides extra mechanical strength and tolerance to the transgenic plants.

Materials and methods

Development of transgenic plants

Full length cDNAs of *PaSOD*, (GenBank accession EU532614.1) and *RaAPX*, (GenBank accession DQ078123.2) from *P. atrosanguinea* and *R. australe*, respectively were overexpressed in *Arabidopsis thaliana* (Ecotype Columbia 0) as described earlier by Gill et al. (2010a). For screening of transgenics, the seeds were surface sterilized, rinsed with sterile water and stratified at 4 °C for two days on half-strength Murashige and Skoog (½ MS; 1962) medium supplemented with 1 % agar, 1 % sucrose and 20 $\mu\text{g ml}^{-1}$ hygromycin. Homozygous (T3 generation) transgenic *PaCuZn-SOD* and *RaAPX* plants were crossed to obtain dual transgenics. Putative transgenics were screened through PCR using gene specific primers (Supplementary Table S1). Single copy gene insertion of each of *Cu/Zn-SOD* and *APX*, in transgenics was determined in the T₂ Generation. The results were statistically

analyzed by χ^2 Test. For Southern hybridization analysis, 30 μg genomic DNA from each transgenic line was digested with *Hind*III and electrophoresed on 0.8 % agarose gel followed by denaturation and transfer to nylon membrane by capillary blotting. Hybridization was carried out with biotin-labeled cDNA probe of either *PaSOD* or *RaAPX* (Sambrook and Russel 2001).

Gene-specific semi-quantitative RT-PCR

Total RNA was isolated from transgenics and WT plants using *iRIS* solution (Ghawana et al. 2007). One micrograms of total RNA was used for oligo (dT) primed first-strand cDNA synthesis in 20 μl reaction using of Superscript III reverse transcriptase (Invitrogen). This cDNA was used in 27 cycle PCR using gene specific primers for *PaSOD* and *RaAPX* genes.

Plant growth and salt stress

Seeds of transgenic lines (T3) over-expressing *PaSOD* (S26, S15), *RaAPX* (APX20, APX2), both genes (180, 19c) and WT were germinated as described above. The seedlings were transplanted to the soil mixture of vermiculite: peat moss: perlite (1:1:1) in the greenhouse under a 16 h light and 8 h dark cycle at 20 ± 1 °C and light intensity of 60–70 $\mu\text{mol PPFd m}^{-2} \text{s}^{-1}$ and irrigated with $\frac{1}{2}$ MS salts, weekly. For stress treatment, 21 days old seedlings of WT, and transgenics were supplemented with desired concentration of NaCl (0, 50, 100 and 150 mM) dissolved $\frac{1}{2}$ MS salts. Three biological replicates were collected from each sample at respective time points after salt stress treatment.

SOD and APX enzyme activity assay

Leaf samples (100 mg) were homogenized in a pre cooled mortar in homogenizing buffer containing 2 mM EDTA, 1 mM DTT, 1 mM PMSF, 0.5 % (v/v) Triton-X100 and 10 % (w/v) PVPP in 50 mM phosphate buffer pH 7.8. For APX activity, homogenizing buffer contained ascorbate in addition and the buffer pH was set to 7.0. The homogenate was transferred to 1.5 ml tubes and centrifuged at 13,000 rpm for 20 min at 4 °C. The supernatant was collected and total SOD and APX activities were estimated. The total SOD activity was measured by adding 5 μl enzyme extract to reaction mixture (200 μl) containing 1.5 μM riboflavin, 50 μM NBT, 10 mM DL-methionine and 0.025 % (v/v) triton-X100 in 50 mM phosphate buffer. One unit of enzyme activity was defined as the amount of enzyme required for 50 % inhibition of NBT reduction per min at 25 °C. Specific activity of SOD was calculated accordingly. APX activity was determined by following the oxidation rate of ascorbate at 290 nm as described by

Nakano and Asada (1981). Protein content was estimated according to the dye binding method of Bradford using BSA as standard (Bradford 1976).

Estimation of electrolyte leakage, relative water content, total soluble sugars and proline content

Electrolyte leakage was measured using an electrical conductivity meter as described by Lutts et al. (1996). Briefly, leaves were excised and washed with deionized water. After drying with filter paper, 1 g fresh weight of leaves were cut into small pieces (about 1 cm^2) and immersed in 20 ml deionized water and incubated at 25 °C. After 24 h, electrical conductivity (EC1) of the bathing solution was recorded. These samples were then autoclaved at 120 °C for 20 min to completely kill the tissues and release all electrolytes. Samples were then cooled to 25 °C and the final electrical conductivity (EC2) was measured. The electrolyte leakage (EL) was expressed following the formula:

$$\text{EL} = \text{EC1}/\text{EC2} \times 100.$$

Relative water content (RWC) was measured according to Barrs and Weatherley (1962). Fully expanded terminal leaflets of second and third leaves from apex were excised and fresh weight (FW) was immediately recorded in between 9 a.m. and 10 a.m.; then the leaves were soaked for 12 h in distilled water at room temperature under constant light and the turgid weight (TW) was recorded and after drying for 48 h at 60 °C total dry weight (DW) was recorded. RWC was calculated according to following equation:

$$\text{RWC} (\%) = [(\text{FW}-\text{DW})/(\text{TW}-\text{DW})] \times 100.$$

Total soluble sugar (TSS) content was determined calorimetrically by the anthrone method (Irigoyen et al. 1992). Free proline content was estimated using the acid ninhydrin method described by Bates et al. (1973).

Determination of H_2O_2 content

The level of H_2O_2 was measured following Sonja et al. (2002) method with some modifications. *Arabidopsis* leaves (100 mg) were ground to a fine powder in liquid nitrogen and the powder was extracted in 2 ml 1 M HClO_4 . Extraction was performed in the presence of insoluble PVP (5 %). Homogenates were centrifuged at 12,000 $\times g$ for 10 min at 4 °C and the supernatant was neutralized with 2.5 M K_2CO_3 to pH 5.6 in the presence of 100 μl 0.1 M phosphate buffer (pH 5.6). The homogenate was centrifuged at 12,000 $\times g$ for 1 min to remove KClO_4 . The sample was incubated prior to assay for 10 min with 1 U ascorbate oxidase (Sigma Aldrich, India) to oxidize ascorbate. The reaction mixture consisted of 0.1 M phosphate buffer (pH

6.5); 3.3 mM DMAB; 0.07 mM MBTH and 50 ng POX (Sigma Aldrich, India). The reaction was initiated by addition of an aliquot (50 or 100 μ l) of the sample. The absorbance change at 590 nm was monitored at 25 °C. For each assay, H₂O₂ contents in the extract were quantified by reference to an internal standard (1.5 nmol H₂O₂, added to the reaction mixture on completion of the absorbance change due to the sample).

Microscopy

For confocal microscopic analysis, inflorescence stems of WT and transgenic lines were harvested and fixed in formalin, glacial acetic acid and ethyl alcohol (FAA, 1:1:18) at room temperature. Sections of 8–10 μ m thickness were cut and stained with 1 % safranin and 4 % fast green. These sections were mounted and examined using Confocal Laser Scanning Microscope (Zeiss LSM510 meta GmbH, Germany). For SEM analysis, segments from the apical 1 cm of stem cross-sections were fixed in a mixture of 2 % paraformaldehyde and 2.5 % glutaraldehyde in 0.1 mol/l cacodylate buffer, pH 7.4 for 1 h and then with 1 % OsO₄ in 0.1 mol/l cacodylate buffer, pH 7.4 for 30 min. After critical point drying, the samples were sputter-coated with gold, and the coated samples were viewed with a Hitachi S-3400N field emission SEM using an accelerating voltage of 30 kV. For TEM study, stem slices were fixed in 4 % (w/v) paraformaldehyde and 1 % (v/v) glutaraldehyde in 0.1 mM phosphate buffer, pH 7.2, for 4 h at room temperature and then postfixed in 1.33 % OsO₄ in cacodylate buffer, pH 7.2, and stained with 1.5 % uranyl acetate. All samples were dehydrated in acetone series, followed by propylene oxide. Embedment was in Araldite, Epon, and dodecyl succinic anhydride in proportions 1:1:3. Polymerization was carried out at 80 °C, and micrographs were taken with a Tecnai G² TF20 electron microscope (FEI, Netherlands).

Histochemical staining

For phloroglucinol-HCl staining, sections of *Arabidopsis* inflorescence were stained with 1 % phloroglucinol (w/v) in 12 % HCl for 5 min and observed under light microscope. Syringyl lignin was stained with the Mäule reagent. Sections were incubated in 0.5 % (w/v) KMnO₄ for 10 min and then in 4 N HCl for 5 min. Stained sections were mounted in the presence of concentrated NH₄OH and observed under a dissection microscope.

Lignin content and composition analysis

Lignin was quantified by modified method of Liyama and Wallis (1990) and using the Klason method (Kirk and Obst

1988). Basal portions of the cuttings (about 2-cm-long), were weighed and 40 mg of lyophilised tissue was placed in test tubes with 2 ml of 80 % (v/v) ethanol. Segments were extracted with three successive 1.5 h extractions in 3 ml of 80 % (v/v) ethanol at 80 °C, followed by 1 h extraction in 3 ml of chloroform at 62 °C. Segments were then dried for 2 days at 50 °C. Dried segments were digested in 2.6 ml of 25 % (v/v) acetyl bromide in acetic acid containing 2.7 % (v/v) perchloric acid. After 1 h, 100 μ l of each sample were added to 580 μ l of a solution of 17.24 % (v/v) 2 N NaOH and 82.76 % (v/v) acetic acid and 20 μ l of 7.5 mol/l hydroxylamine hydrochloride were added to ensure termination of the reaction. The volume was corrected to 2 ml with acetic acid and the absorbance at A280 was measured. Lignin was expressed as mg/g fresh weight.

For Klason lignin, stems were ground into fine powder. After four extractions in methanol and vacuum drying, 200 mg of the sample was hydrolyzed in 4 ml of 72 % H₂SO₄ at 30 °C for 1 h. The hydrolysate was diluted by the addition of 112 ml of H₂O and then autoclaved for 1 h. The sample solution was filtered through a fritted glass crucible. The sample was washed and dried, and then lignin was measured and expressed as a percentage of the original weight of cell wall residues (% CWR).

Composition of lignin was analyzed following the method by Akin et al. (1993). Briefly, the ethanol-extracted stem samples were hydrolyzed in 4N NaOH at 170 °C for 2 h. The hydrolysate was acidified with 2N HCl to pH 2.0. The released lignin monomers were extracted into diethylether and vacuum dried. The residue was dissolved in 10 ml of pyridine and 10 ml of *N, O*-bis(trimethylsilyl) trifluoroacetamide and analyzed for phenolics by gas-liquid chromatography. Compounds were identified by comparison of their mass spectra with published spectra or those of the authentic compounds. All samples were run in duplicate.

Statistical analysis

All experiments were conducted with at least three independent repetitions in triplicates. All values are shown as the mean \pm the standard deviation. The statistical analysis was performed using Statistica software (v.7). The statistical significance between the mean values was assessed by analysis of variance (ANOVA) applying Duncan's Multiple Range Test (DMRT). A probability level of $P \leq 0.05$ was considered significant.

Transcriptome sequencing, assembly and annotation

RNA-seq libraries were made from 2 μ g RNA from each of these samples using TruSeq RNA sample prep kit (Illumina) as per manufacturer's instruction. Libraries were quantified using QubitTM dsDNA High Sensitivity assay kit

for Qubit 2.0[®] Fluorometer (Life Technologies, USA) and with an Agilent Bioanalyzer chip DNA 1000. Each library had an average insert size of 200 bp and 10 pM of the prepared library were loaded onto a flowcell for cluster generation. PE 2 × 72 bp sequences were generated on Illumina genome analyzer IIx following manufacturer's instructions. Paired end (PE) sequence reads of length 72 bp each were generated using CASAVA package provided by Illumina. Quality assessment of reads was done using read quality filtering tool, filterR with minimum quality score threshold of 30 QS. Reads where 70 % of bases scored above the threshold quality score were taken into consideration (Gahlan et al. 2012). In the current study, TAIR10 genome release of *A. thaliana* was used as reference while TopHat and Cufflinks protocol were used for reference based assembly and annotation of assembled transcripts (Trapnell et al. 2012). The assembled transcripts were annotated using Cuffcompare version 2.0.2. The TAIR10 GTF (Gene Transfer Format) file of *A. thaliana* was used for annotation based on available species information. All the assembled transcripts were also searched against UniProt databases at an e-value threshold of 10⁻¹ to perform annotations based on sequence similarity (<http://www.uniprot.org/downloads>). The associated GO, KEGG and EC annotations were derived using Annot8r (Schmid and Blaxter 2008). The assembled transcripts were searched against this database using BLASTX at an E-value threshold of 10⁻⁵ (Altschul et al. 1990).

Quantitative real-time PCR analysis (qRT-PCR)

Total RNA was pretreated with RNase-free DNase I (Invitrogen, USA) followed by first strand cDNA synthesis with 2 µg of total RNA using superscript III (Invitrogen, USA) according to the manufacturer's instructions. Gene specific primers (Supplementary Table S1) were designed using Primer 3 software (Rozen and Skaletsky 2000) and a β-actin gene (AT3G18780) was used as the endogenous control as suggested (Czechowski et al. 2005). Gene expression was performed on a Stratagene Mx3000P system (Agilent Technologies, Germany) using 2× Brilliant III SYBR Green qPCR Master Mix (Agilent Technologies, Germany). All qPCRs were run in triplicates with a no-template control to check for contamination. PCR was conducted under the following conditions: 10 min at 95 °C (enzyme activation), 40 cycles each of 30 s at 95 °C, 30 s at 55 °C and 72 °C for 30 s and a final melting curve analysis was performed (55–95 °C) to verify the specificity of amplicons. The dissociation curves showed that the primers used for qRT-PCR were gene-specific. The raw threshold cycle (Ct) values were normalized against a reference gene encoding Actin to calculate relative expression in salt stress treated samples with respect to control using the Relative Expression Software Tool (REST; Pfaffl et al. 2002).

Expression values were log₂ transformed and Heat maps were generated and hierarchical clustering done using the Institute for Genomic Research (TIGR) MeV v4.4.1 software package.

Results

Overexpression of *PaSOD* and *RaAPX* in *Arabidopsis*

In total, 9 independent lines for *PaSOD* and 20 independent lines for *RaAPX* were found to be PCR positive (Supplementary Figure S1A–C). PCR positive lines were subjected to χ^2 Test (Supplementary Table S2) and on the basis of 3:1 ratio, transgenic lines having single copy number were determined. The single copy integration of respective transgene(s) in S15, S26, APX2, APX20, 18O and 19c lines, which were used for further analyses, was re-confirmed through Southern hybridization analysis. All these lines were found to have single copy insertion of the transgene (Supplementary Figure S2). The SOD and APX activities were estimated in *PaSOD* and *RaAPX* overexpressing lines, respectively and it was observed that S15, S26, APX2, APX20, 18O and 19c showed high SOD and APX activity among respective transgenic lines (Supplementary Figure S3A, B). On the basis of single copy insertion of respective transgene and maximum activity of SOD or APX, S26 (*PaSOD*-overexpressing) and APX20 (*RaAPX*-overexpressing) lines were selected for generation of dual transgenics. In total, four independent dual transgenic lines were generated. Expression of respective transgenes in S15 and S26 (*PaSOD* lines), APX2 and APX20 (*RaAPX* lines) and 18O and 19c (dual transgenic lines) was confirmed through RT-PCR analysis (Supplementary Figure S4A, B).

Effect of salt stress on antioxidant enzyme activities

Total enzyme activities of SOD and APX were estimated in WT and transgenic samples collected at 1 and 24 h of salt stress. Enzyme assays for total SOD and APX revealed that their activities increased with increase in magnitude of salt stress in WT and all the transgenic plants. Total enzyme activities increased gradually up to 100 mM NaCl and then decreased at 150 mM NaCl in WT and all the transgenic lines, after which the minimal levels were maintained. However, total SOD and APX activities were significantly higher in transgenic plants as compared to WT under control as well as under salt stress, as the genes were overexpressed under constitutive CaMV35S promoter (Fig. 1a, b; Supplementary Table S3). The increase in total SOD activity was 1.8 to 2 fold higher in *PaSOD* lines and 2.6 fold in dual transgenic lines as compared

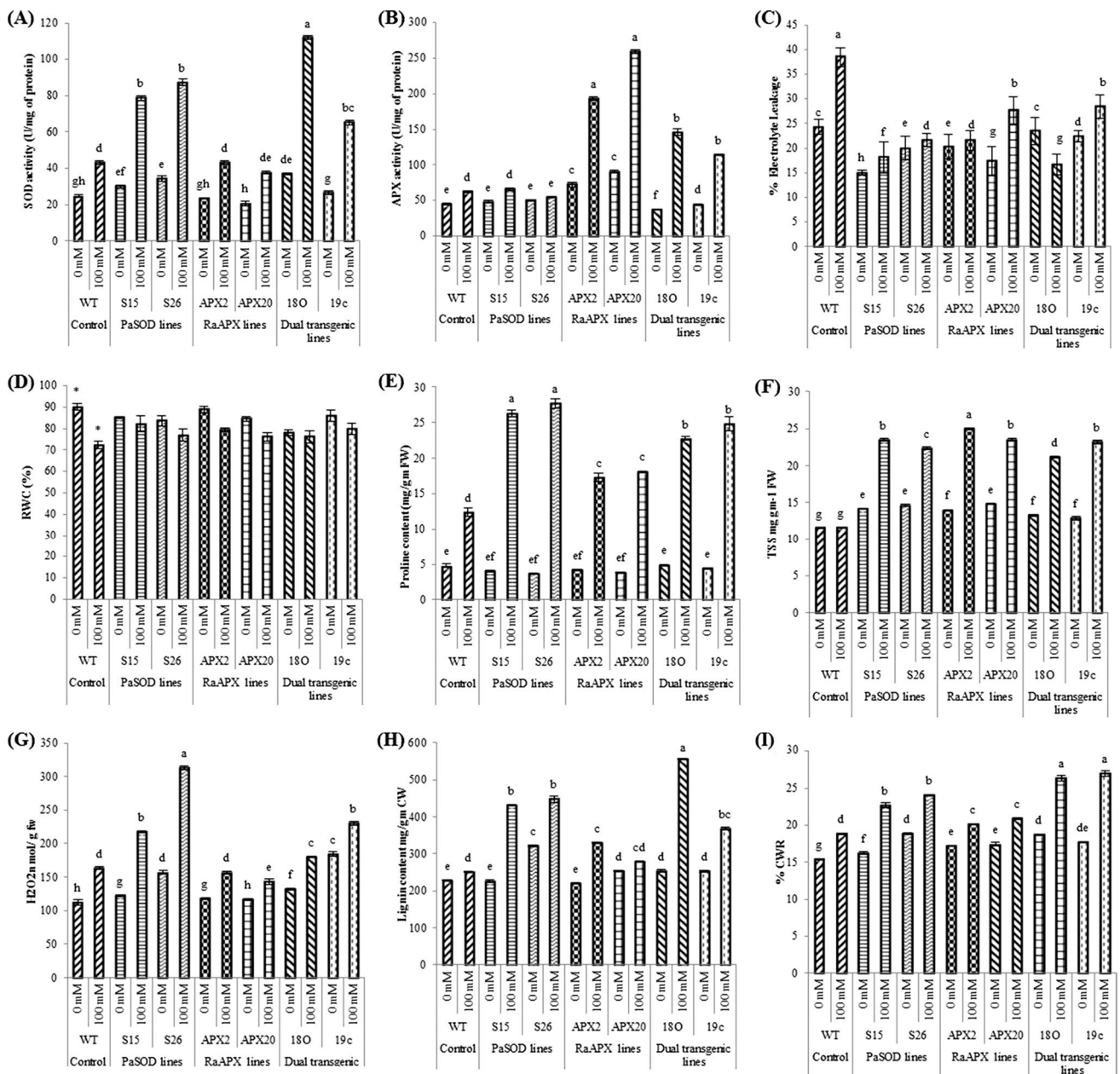


Fig. 1 Biochemical analysis of WT and transgenic lines under control and stress conditions salt stress. **a** Superoxide dismutase (SOD) enzyme activity. **b** Ascorbate (APX) enzyme activity. **c** Percentage electrolyte leakage. **d** Percentage relative water content (RWC). **e** Proline content. **f** Total soluble sugar content. **g** H₂O₂ content. **h**

lignin content. **i** Klason lignin. Data represent the mean \pm SE of three independent experiments ($n = 3$). Different letters on top of the bars indicate significant difference at a level of $P < 0.05$, as determined by Duncan's multiple range test (DMRT)

to WT, under 100 mM NaCl treatment (Fig. 1a). Nearly 2.5–4.3 fold increase in APX activity was observed in RaAPX lines and 1.7–1.8 fold in dual transgenic lines as compared to WT under 100 mM NaCl treatment. But the levels of APX activity were higher throughout the stress in transgenic plants, especially in APX20 where nearly three fold higher activity was recorded (Fig. 1b; Supplementary Table S3).

Response of transgenics under salt stress

The transgenic lines showed better performance under salt stress in terms of growth parameters such as, plant height, root length, rosette area and number of leaves (Supplementary Table S4) as compared to WT. Several yield parameters such as size of pod, number of pods and total seed yield were also higher in transgenic lines than

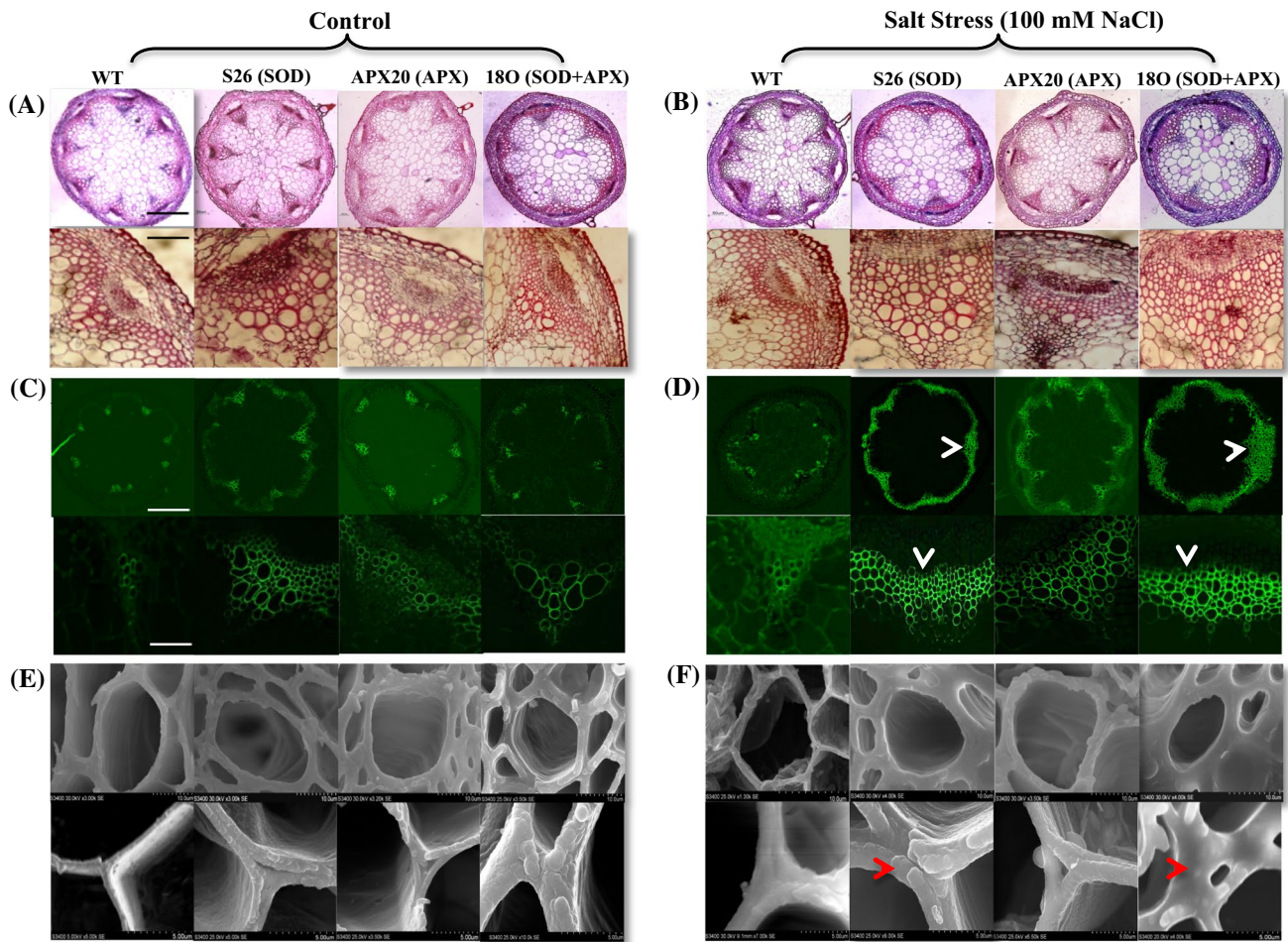


Fig. 2 Histochemical analysis of lignin in the stem of *Arabidopsis*. **a, b** Transverse stem sections were stained with safranin-O for lignin. **c, d** Lignification pattern under control and salt stress. *Lower panel* is the close up view of the single vascular bundle and *white arrows* show enhanced lignification. **e, f** Sections observed under scanning

electron microscope, *red arrows* show wall thickening. *Bar* in **a, b** upper panel 100 μm and *bar* in **a, b** lower panel 50 μm . *Bar* in **c, d** upper panel 90 μm and *bar* in **c, d** lower panel 56 μm . *Bar* in **e, f** upper panel 10 μm and *bar* in **e, f** lower panel 5 μm

WT. Electrolyte leakage analysis revealed that, there was no significant difference in electrolyte leakage in WT and transgenic lines under control conditions. Under salt stress, electrolyte leakage was found to be significantly lower in transgenic lines as compared to WT plants (Fig. 1c). Among transgenic lines, least electrolyte leakage was found in 180 line under salt stress. Relative water content (RWC) was observed to be similar in both, WT and transgenics under control conditions. However under salt stress, WT suffered significant reduction in RWC as compared to transgenic lines. In all transgenic lines, the reduction in RWC was not significant at all tested NaCl concentrations (Fig. 1d). The transgenic lines under salt stress possess increased levels of proline and soluble sugars. The accumulation of proline was two fold higher in *PaSOD* lines, 1.4 fold in *RaAPX* lines and 1.8–2 fold in dual transgenic lines as compared to WT (Fig. 1e). Soluble sugar

content was also significantly higher (two fold) in all the transgenic lines as compared to WT, where no significant change in soluble sugar levels was observed at the same salt stress conditions (Fig. 1f). Our results suggest that the higher tolerance of the transgenic lines to salt stress is a result of the accumulation of more proline and total soluble sugars as compared to WT.

Effect of salt stress on H_2O_2 and ROS accumulation

H_2O_2 contents in WT and transgenic lines at different salt concentrations were estimated. Under control conditions, H_2O_2 content of WT and transgenic lines exhibited the same trend, while under salt stress conditions, enhanced H_2O_2 accumulation was observed in all transgenic lines with higher amounts detected in *PaSOD* (1.2–2.3 fold) and dual transgenic lines (1.1–2 fold) followed by *RaAPX*

Table 1 Wall thickness of vessels and fibers in stems of the WT and transgenic lines

Lines	Sample	Interfascicular fibers (μm)	Vessels (μm)	Xylary fibers (μm)
<i>Control</i>				
WT	0 mM NaCl	2.97 \pm 0.09 ^{def}	0.86 \pm 0.03 ^{ef}	0.19 \pm 0.01 ^f
	50 mM NaCl	2.839 \pm 0.14 ^{bcd}	0.903 \pm 0.03 ^{de}	0.18 \pm 0.03 ^g
	100 mM NaCl	2.19 \pm 0.18 ^g	0.75 \pm 0.02 ^{fg}	0.18 \pm 0.02 ^g
	150 mM NaCl	1.848 \pm 0.14 ^g	0.765 \pm 0.05 ^{fg}	0.155 \pm 0.02 ⁱ
<i>PaSOD lines</i>				
S15	0 mM NaCl	2.611 \pm 0.09 ^{ef}	0.808 \pm 0.02 ^{efg}	0.261 \pm 0.02 ^e
	50 mM NaCl	3.334 \pm 0.06 ^{bc}	1.293 \pm 0.02 ^b	0.313 \pm 0.02 ^d
	100 mM NaCl	3.305 \pm 0.04 ^{bcd}	0.899 \pm 0.01 ^{de}	0.321 \pm 0.02 ^d
	150 mM NaCl	2.821 \pm 0.17 ^{ef}	0.696 \pm 0.03 ^g	0.188 \pm 0.01 ^g
S26	0 mM NaCl	2.81 \pm 0.17 ^{ef}	0.80 \pm 0.02 ^{efg}	0.24 \pm 0.02 ^{de}
	50 mM NaCl	3.38 \pm 0.06 ^{bcd}	1.27 \pm 0.01 ^b	0.43 \pm 0.01 ^c
	100 mM NaCl	3.47 \pm 0.15 ^{bc}	0.89 \pm 0.01 ^{de}	0.30 \pm 0.01 ^d
	150 mM NaCl	2.82 \pm 0.17 ^{ef}	0.696 \pm 0.02 ^g	0.18 \pm 0.01 ^g
<i>RaAPX lines</i>				
APX2	0 mM NaCl	2.545 \pm 0.08 ^f	0.768 \pm 0.02 ^{fg}	0.175 \pm 0.01 ^h
	50 mM NaCl	2.934 \pm 0.10 ^{def}	0.901 \pm 0.01 ^{de}	0.397 \pm 0.02 ^c
	100 mM NaCl	3.319 \pm 0.05 ^{bc}	0.808 \pm 0.01 ^{efg}	0.269 \pm 0.01 ^{de}
	150 mM NaCl	2.155 \pm 0.15 ^g	0.731 \pm 0.03 ^g	0.149 \pm 0.01 ^{ij}
APX20	0 mM NaCl	2.64 \pm 0.10 ^f	0.75 \pm 0.02 ^{fg}	0.17 \pm 0.01 ^h
	50 mM NaCl	3.00 \pm 0.12 ^{def}	0.89 \pm 0.01 ^{de}	0.42 \pm 0.01 ^c
	100 mM NaCl	3.20 \pm 0.13 ^{cde}	0.7308 \pm 0.02 ^g	0.23 \pm 0.02 ^e
	150 mM NaCl	2.15 \pm 0.13 ^g	0.783 \pm 0.03 ^{fg}	0.14 \pm 0.01 ^k
<i>Dual (PaSOD +RaAPX) transgenic lines</i>				
18O	0 mM NaCl	3.36 \pm 0.05 ^{bcd}	1.13 \pm 0.03 ^c	0.29 \pm 0.04 ^{de}
	50 mM NaCl	3.78 \pm 0.20 ^b	1.00 \pm 0.05 ^d	0.58 \pm 0.01 ^b
	100 mM NaCl	4.83 \pm 0.16 ^a	1.41 \pm 0.01 ^a	0.62 \pm 0.02 ^a
	150 mM NaCl	3.47 \pm 0.08 ^{bc}	0.80 \pm 0.02 ^{efg}	0.26 \pm 0.01 ^{de}
19c	0 mM NaCl	3.261 \pm 0.03 ^{bcd}	1.036 \pm 0.01 ^c	0.198 \pm 0.06 ^{fi}
	50 mM NaCl	3.723 \pm 0.18 ^b	1.029 \pm 0.05 ^d	0.568 \pm 0.01 ^b
	100 mM NaCl	4.45 \pm 0.08 ^a	1.425 \pm 0.01 ^a	0.637 \pm 0.01 ^a
	150 mM NaCl	3.204 \pm 0.13 ^{cde}	0.783 \pm 0.03 ^{fg}	0.23 \pm 0.03 ^e

Wall thickness was measured from electron micrographs of fibers and vessels. Data are mean (μm) \pm SE from cells. Means were compared using ANOVA. The letters a, b, c, and d indicates significant differences at the level of $P > 0.05$, as determined by Duncan's multiple range test (DMRT)

(0.5–1.7 fold; Fig. 1g). In situ detection of H_2O_2 was performed, where intensity of brown color correlates with the levels of H_2O_2 accumulation (Supplementary Figure S5A). Under control conditions, WT and transgenic lines showed a very low H_2O_2 accumulation. While at 150 mM NaCl, H_2O_2 accumulation was found to be highest in WT followed by S26, APX20 and 18O. The H_2O_2 accumulation at 50 and 100 mM NaCl, was found to be lower in transgenic lines than WT. In situ detection of ROS showed that the amount of O_2^- (ROS) increased significantly with higher degree of salt stress in WT and transgenic lines. However, the O_2^- content was found to be higher in WT as compared to transgenic lines under salt stress. At higher levels of salt stress (100 and 150 mM), the S26 and 18O lines showed least O_2^- content amongst the transgenic lines (Supplementary Figure S5B).

Anatomical alterations of transgenics

Lignin provides mechanical strength to water conducting vessel elements. To ascertain whether an increase in lignin could significantly affect the wall strength, we examined the anatomy of vessels. Anatomical investigations revealed drastic anatomical changes in the stem of transgenic lines as compared to WT under salt stress. Interfascicular lignification was evident even under control conditions and lignification enhanced under NaCl stress in all transgenics, whereas stem of WT showed lignin deposition in the vascular bundles only (Fig. 2a, d; Supplementary Figure S6A–D). In S26 and 18O lines, lignification of the interfascicular arcs was conspicuous along the entire stem, and vascular bundles were connected by lignified arcs under stress condition (Fig. 2d; Supplementary Figure S6D). Cell walls

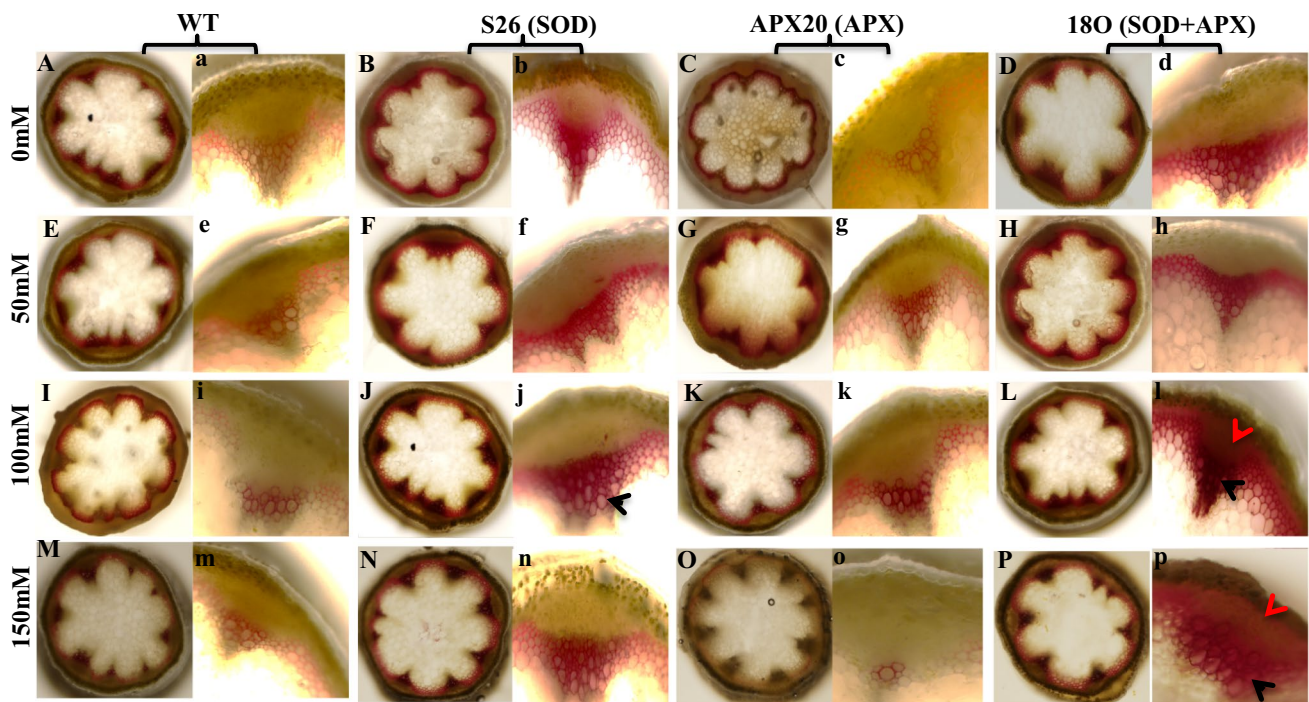


Fig. 3 Overexpression of SOD and APX leads to enhanced lignin deposition in stem of *Arabidopsis*. Stem sections were stained with phloroglucinol-HCl (Wiesner stain) for detection of lignin rich in G (guaiacyl) monolignol subunit. Bar 90 μ m for A–P, and bar 56 μ m in a–p. **Aa, Ee, Ii** and **Mm** WT stem cross sections showing the normal lignin deposition. **Bb, Ee, Jj** and **Nn** S26 stem section (*dark purplish red color*) showing enhanced lignin deposition (*black arrow*). **Cc,**

Gg, Kk and **Oo** APX20 stem cross sections (*red color*) showing the normal lignin deposition. **Dd, Hh, Ll** and **Pp** 180 stem section showing ectopic lignin deposition (*dark purplish red color*) in the walls of cortical and epidermal cells (*red arrow*), in addition to enhanced deposition of lignin (*black arrow*) in inter-fascicular fibers and xylem cells

of vascular bundles in transgenic lines were much thicker and larger compared to WT as observed in electron micrographs (Fig. 2e, f; Supplementary Figures S6E, F, S7). The increased thickness of inter-fascicular fibers, vessels and xylary fibers was due to enhanced lignification. Thus the increase in height of transgenic plants (Supplementary Table S4), compared with WT plants was primarily caused by increased length of xylem fiber cells (Table 1). We also assayed the lignification in the stems of WT and transgenics using phloroglucinol stain (for p-hydroxycinnamaldehyde end groups) and the Mäule reaction (for detection of syringyl S moieties). Lignin was revealed by Wiesner staining in inter-fascicular fibers and xylem bundles of WT and transgenic stems. In transgenic stems, variation (lighter to darker) in the coloration was revealed, because of changes in lignin composition. Lignin was stained as a bright violet-red color principally through reactions involving coniferaldehyde end groups. The staining of stems of S26 and 180 lines was significantly darker than WT plants, suggesting that the transgenic plants contained more 4-O-linked hydroxycinnamyl aldehydes. Further, ectopic lignin deposition was observed in the walls of cortical and epidermal cells of 180 at 100 mM and 150 mM NaCl (Fig. 3I,

p; Supplementary Figure S8I, p). The Mäule staining displayed red/orange staining in the xylem and inter-fascicular regions of WT and transgenics under stress and control conditions, but was extensively seen in vascular tissues of 180 (Fig. 4L, l). Mäule staining of 180 plants also showed a change in color from dark-brown to wine-red (Fig. 4D, H, L, P; Supplementary Figure S9D, H, L, P), indicating an increase in S content. This observation suggests that the 180 line is rich in S lignin and 100 mM salt stress induces higher lignification.

Effect of transgene overexpression on lignin content and composition

To investigate the effect of overexpression of these antioxidant genes on lignin content and composition, mature stems of the WT, *PaSOD* (S15 and S26), *RaAPX* (APX2 and APX20) and dual (180 and 19c) transgenic lines were used for lignin estimation under different salt stress conditions. With the increase in salt concentration, the lignin content also increased; indicating active lignin synthesis during stress conditions (Supplementary Table S3). The lignin content of transgenics was significantly higher than

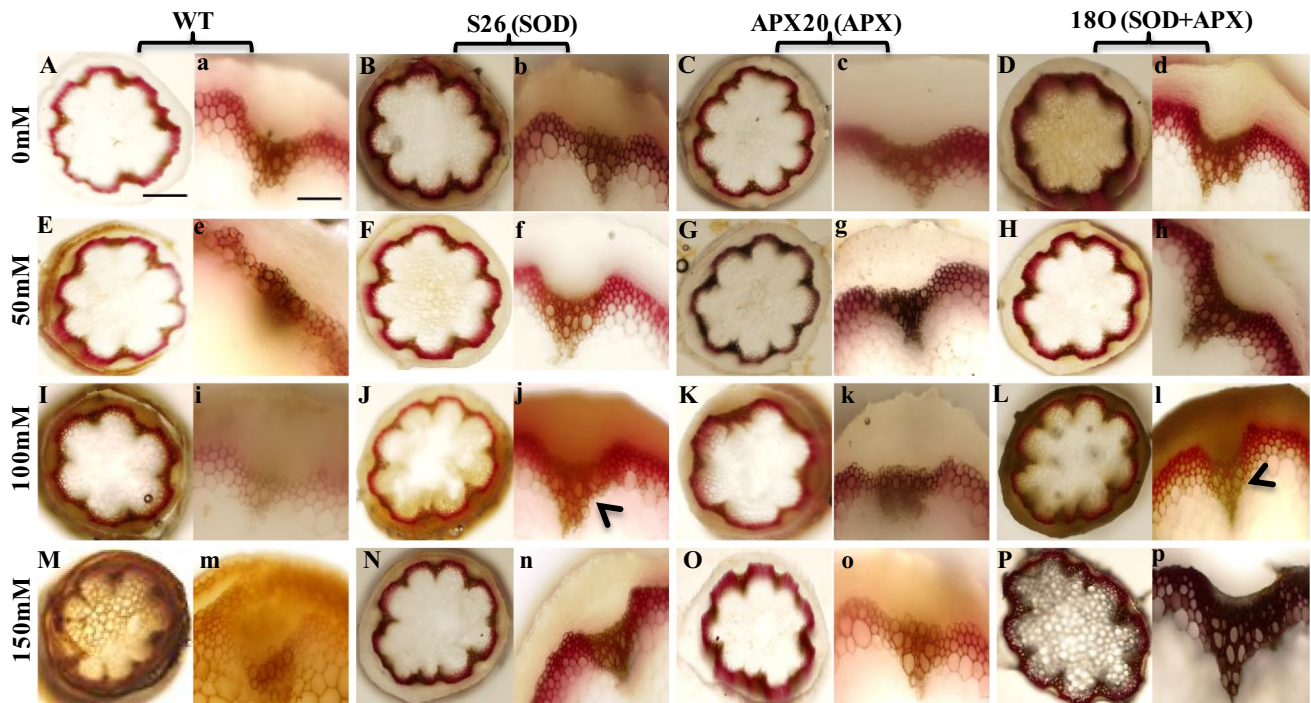


Fig. 4 Mäule staining of lignin in transverse sections of *Arabidopsis* stem to detect lignin rich in guaiacyl (G) and syringyl (S) monolignol subunits. Bar 90 μm for A–P and bar 56 μm in a–p. Aa, Ee, Ii and Mm WT stem sections (brown color) showing the normal lignin deposition. Bb, Ee, Jj and Nn S26 stem section showing change in color

from dark brown to red (black arrow). Cc, Gg, Kk and Oo APX20 stem sections (brown color) showing the normal lignin deposition. Dd, Hh, Ll and Pp 180 stem sections showing change in colour from dark brown to red (black arrow) in the walls of interfascicular fibers and xylem cells

Table 2 Lignin composition in the stems of the WT and transgenic lines

Plant	G Lignin	S Lignin	Total G and S lignin
WT, 0 mM	2.66 \pm 0.78 ^c	1.09 \pm 0.37 ^c	3.75 (100 %)
WT, 100 mM	2.02 \pm 0.19 ^c	0.67 \pm 0.13 ^d	2.69 (71.73 %)
S26, 0 mM	5.25 \pm 1.9 ^{bc}	2.72 \pm 1.08 ^a	7.97 (212.54 %)
S26, 100 mM	6.34 \pm 1.02 ^a	1.74 \pm 0.70 ^b	8.08 (215.47 %)
APX, 0 mM	4.34 \pm 1.35 ^{bc}	1.62 \pm 0.34 ^b	5.96 (158.94 %)
APX, 100 mM	4.77 \pm 0.93 ^{bc}	0.93 \pm 0.25 ^c	5.70 (152 %)
180, 0 mM	5.84 \pm 0.14 ^{ab}	2.37 \pm 0.36 ^a	8.21 (218.93 %)
180, 100 mM	6.50 \pm 1.75 ^a	2.84 \pm 0.71 ^a	9.34 (249.07 %)

The monolignol composition was analyzed according to Akin et al. (1993). Each data point is the mean (mg/g dry cell walls) \pm SE of three separate assays. Means were compared using ANOVA. The letters a, b, c, d indicates significant differences at the level of $P > 0.05$, as determined by Duncan's multiple range test (DMRT). Shown in the parentheses are the percentages of total G and S lignin in SOD and APX overexpressing lines relative to that in the wild type

WT (1.8 fold higher in *PaSOD* lines and 1.6–2 fold in dual lines) at 100 mM NaCl (Fig. 1H). The lignin content estimated through acetyl bromide method was in accordance with the Klason lignin content which showed that lignin content was increased by 13 % in *PaSOD* lines and 14 %

in dual lines as compared to WT under 100 mM NaCl treatment (Fig. 1I). These results indicated that 1.6–2 fold higher lignin deposition led to a major change in vessel wall shapes at 100 mM NaCl. These results are consistent with the histological staining showing more lignifications in the xylem of S26 and 180 lines. The ectopic deposition of lignin in stem was also confirmed by lignin composition analysis which showed that both guaiacyl (two to three folds) and syringyl (2.5–4 folds) lignin contents were elevated in the dual lines as compared to WT (Table 2). The transgenic plants had two to four folds higher total lignin content than WT. Moreover, the transgenic plants had an altered monolignol composition with an increased S:G ratio.

Transcriptome analysis of WT and transgenics under salt stress

In previous section, it was shown that lignin content was higher in transgenic lines as compared to WT under salt stress conditions; it was intriguing to study the expression pattern of various genes associated with lignin biosynthesis. Whole transcriptome profiling was done to determine which genes of lignin biosynthesis pathway are differentially expressed among three types of transgenics lines

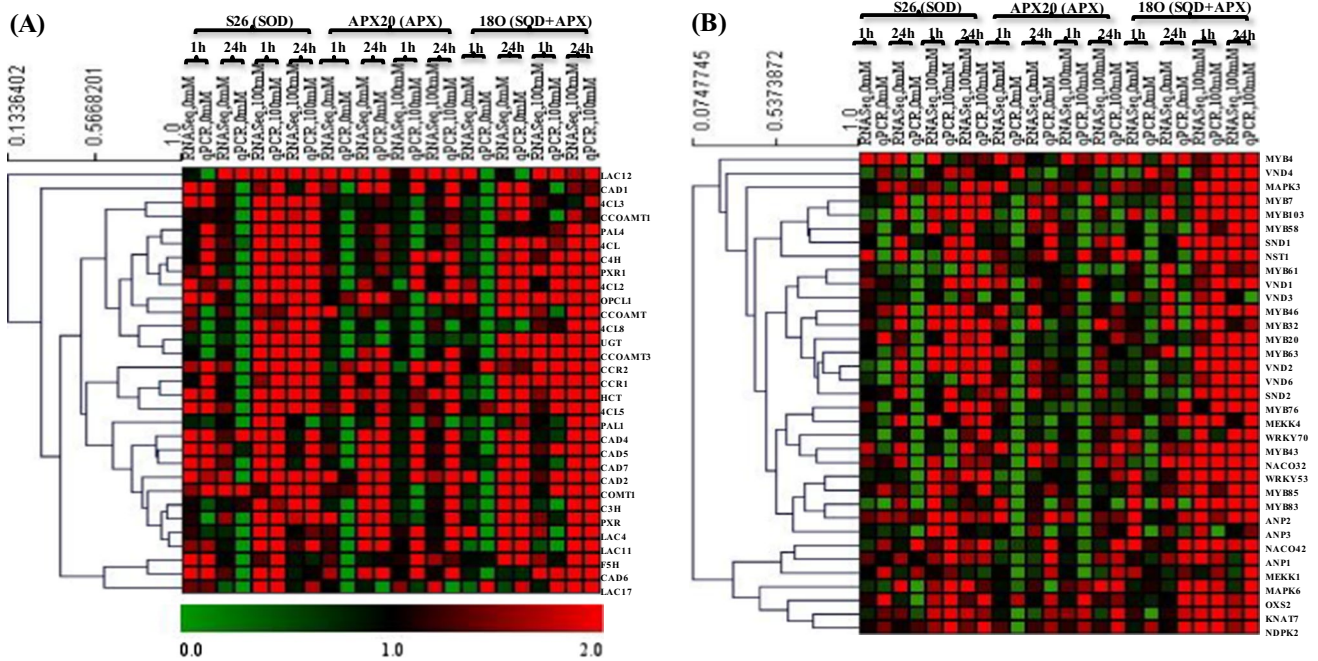


Fig. 5 Heat map showing differential expression of **a** lignin biosynthesis genes and **b** transcription factors involved in lignin biosynthesis under control and salt stress. Heat map represents relative expression ratio of each gene under control and salt stress treatment for 1 and 24 h with respect to WT. The relative expression ratios obtained

under different salt stress conditions. Based on co-expression analysis, lignin biosynthesis genes and certain candidate transcription factors were identified whose expression patterns were correlated with lignification. Using high throughput sequencing on Illumina GAIIx (Supplementary Figure S10), a total of 495,692,298 reads were generated for all the 32 samples (Supplementary Table S5). The read quality score for all the samples was found to be >30 (Supplementary Figure S11). After performing read filtering, a total of 387,748,946 reads were used for reference based assembly using TopHat and Cufflinks protocol. A total of 1,16,778 transcripts were obtained for whole transcriptome of 32 conditions. All the significant differentially expressed transcripts were identified in each comparative condition (Supplementary Table S6) and GO enrichment analysis was performed using AgriGO. It was found that in both the comparative conditions (condition I; 18O, 100 mM NaCl w.r.t. 0 mM at 24 h stress and condition II; 18O w.r.t. WT under 100 mM NaCl at 24 h stress), biological processes belonging to signalling, response to stimulus and the metabolic pathways were highly enriched (Supplementary Figure S12, S13). In condition I, among molecular processes, protein serine/threonine kinase activity (p value $3.96e-12$) and in biological processes response to abiotic stimulus ($6.48e-16$), MAPKKK cascade ($1.05e-26$), regulation/biosynthesis of H_2O_2 metabolic process ($1.82e-15$ to

from RNA-seq data were validated using qRT-PCR with three biological replicates. Bar at the bottom indicates relative expression ratio whereby red, black and green colors represent upregulation, no change and downregulation, respectively

0.00171) and positive regulation of flavonoid biosynthetic process (0.00267) were found to be highly enriched (Supplementary Figure S12). In condition II, under molecular function, protein serine/threonine kinase activity ($2.72e-10$) and transcription factor activity (0.0171) were highly enriched (Supplementary Figure S13). The most abundant TF families observed under stress condition were C3H (6–11 %), MADs (6–8 %), MYB-related (5–8 %), NAC (3–5 %), bHLH (4–6 %) and WRKY (2–4 %). However, bZIP (1–3 %), SNF2 (2–4 %) were also observed, but with relatively less abundance (Supplementary Figures S14, S15).

Transcriptome analysis suggested modulations of lignin biosynthetic pathway

On the basis of gene IDs, 32 genes belonging to lignin biosynthesis pathway were identified and their FPKM based gene expression was validated using qPCR. The data revealed that under control conditions (0 mM NaCl), only few genes showed upregulation in transgenic lines compared to WT. However, a major drift in expression pattern was observed after 24 h of 100 mM salt stress in 18O and S26 transgenic lines and less change was observed in APX20. Most of these genes involved in lignin biosynthesis exhibit upregulation in 18O line after 24 h of salt stress

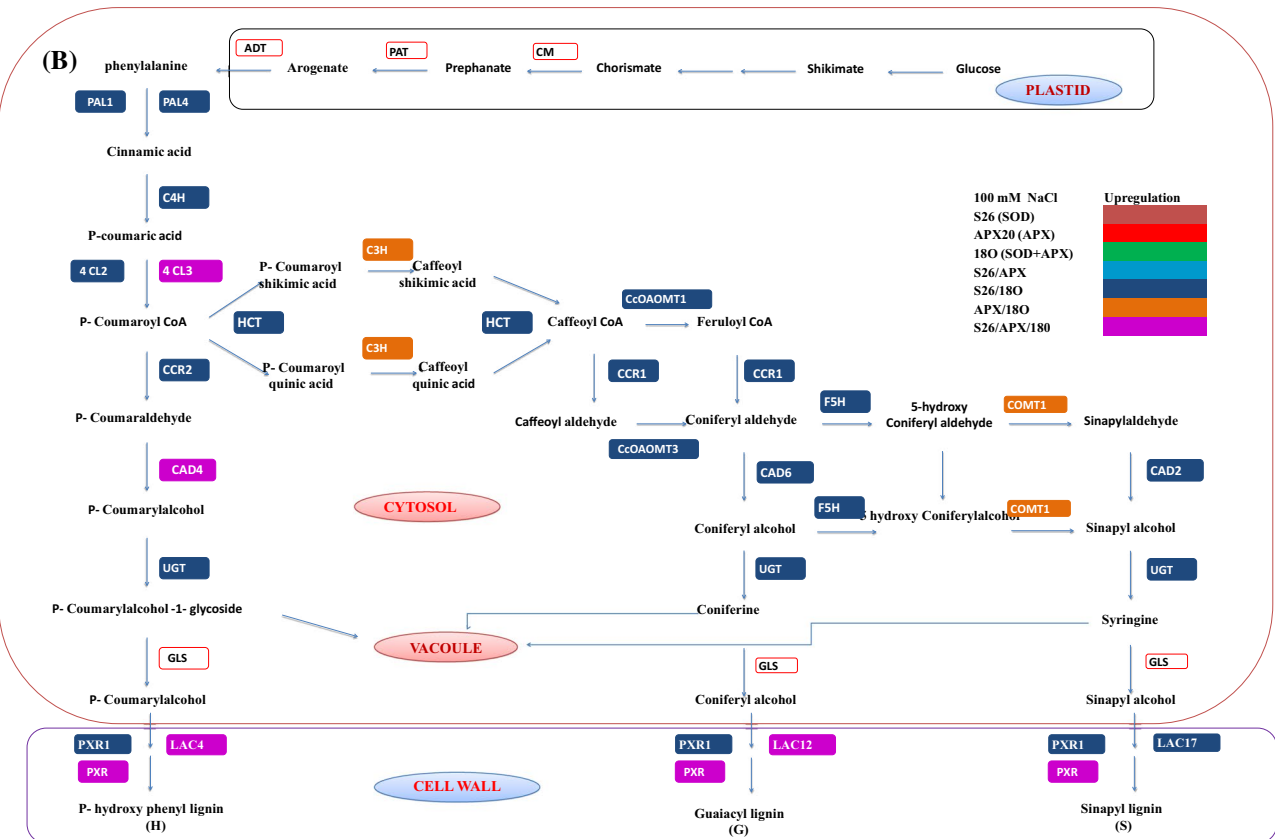
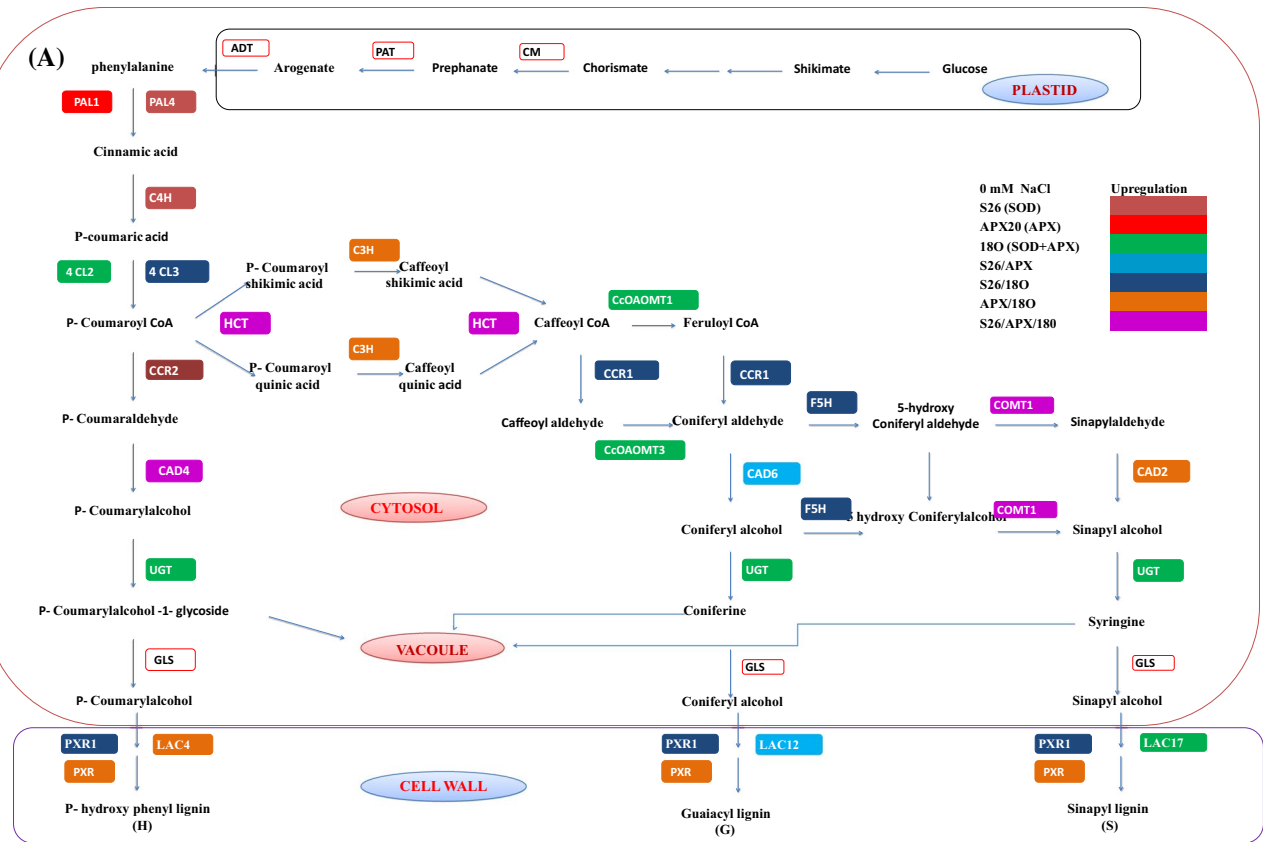


Fig. 6 Overview of monolignol biosynthesis pathway upregulation in WT, S26, APX20 and 18O under Salt Stress (100 mM NaCl) conditions. The “metabolic grid” shown in this scheme incorporates the results of the studies done through RNA-seq and qPCR, it represents the major drift in upregulation pattern under 0 mM (a) and 100 mM (b) salt stress, where major drift in expression pattern occurs at 100 mM salt stress, most of the genes in 18O line shows upregulation followed by S26 and only few genes in APX20 line. Each arrow shows a reaction in the pathway, and next to each arrow is the name of the enzyme that catalyzes the associated reaction, Abbreviations are listed as per pathway. *CM* chorismate mutase, *PAT* prephenate aminotransferase, *AGT* arogenate dehydratase, *PAL* phenylalanine ammonia lyase, *C4H* cinnamate 4-hydroxylase, *4CL* coumarate:CoA ligase, *CCR* cinnamoyl-CoA reductase, *CAD* cinnamyl alcohol dehydrogenase, *HCT* hydroxycinnamoyl-CoA transferase, *C3H* *p*-coumarate 3-hydroxylase, *F5H* ferulate 5-hydroxylase, *COMT* caffeic acid *O*-methyltransferase, *UGT* UDP-glucosyltransferase, *LAC* laccases, *PXR* peroxidases, *CCoAOMT* caffeoyl-CoA 3-*O*-methyltransferase, *H* lignin *p*-hydroxy phenyl lignin, *G* lignin guaiacyl lignin monomers, *S* lignin syringyl lignin monomers

as compared to WT. However, five genes (*CAD1*, *4CL3*, *4CL8*, *LAC12* and *CcAOMT1*) showed downregulation according to both RNA-seq and qPCR data (Fig. 5a; Supplementary Tables S7 to S9). In addition, S26 line also exhibited upregulation of 12 genes of lignin biosynthesis pathway, while rest of the genes were downregulated. In *RaAPX* line (APX20), *4CL1*, *C4H*, *CCR2*, *HCT*, *LAC12*, *CAD1* and *CAD2* genes showed upregulation at 100 mM salt stress. These results indicate that perturbations in lignin biosynthesis pathway occur in response to salt stress with major differences observed in 18O followed by S26 and APX20 lines.

Identification of transcription factors and signalling components regulating lignin biosynthesis

Among the Top 20 most abundant TF families, *C3H* (8.5 %), *MADS* (6.6 %), *PHD* (5.5 %), *MYB*-related (5.3 %), *NAC* (4.86 %), *bHLH* (4.7 %), *WRKY* (3.5 %), *bZIP* (2.1 %) and *MYB* (1.5 %) families were observed (Supplementary Figure S16). In our RNA-seq data, majority of genes belonging to *MYB*, *NAC*, *C3H* and *WRKY* TFs showed changes in the expression in transgenic lines under salt stress as compared to the control as well as to the WT. Among these transcription factors, expression of 32 genes which are directly involved in H₂O₂ signalling and regulation of lignin biosynthesis was validated by qPCR (Fig. 5b). Most of these genes showed upregulation in 18O line under salt stress. Among *VND* (vascular related *NAC*-domain) and *SND* (secondary wall-associated *NAC* Domain) family of transcription factors *VND1*, *VND2*, *VND4*, *VND6*, *SND1*, *SND2* and *NST1* (*NAC* Secondary wall thickening promoting1) showed upregulation, while *VND3* was downregulated (Supplementary Tables S10 to S12). This expression pattern was similar in S26 line, but

in addition to *VND3*, transcription factors *SND2*, *MYB83* and *MYB61* also showed downregulation. *MAPKKK* cascade was found to be highly enriched among biological processes, where *ANP1*, *ANP2* and *ANP3* which are activated by H₂O₂ and its associated downstream signalling network molecules *MAPK3*, *MAPK4*, *MAPK6*, *NDPK2* and *MEKK1* showed change in expression according to both RNA-seq and qPCR analyses. Among these transcription factors and signalling molecules *ANP1*, *MEKK1*, *MEKK4*, *MAPK6* showed upregulation in qPCR whereas, *ANP3* showed downregulation in both RNAseq and qPCR.

Discussion

In this article, we have raised and analyzed transgenic lines overexpressing *PaSOD*, *RaAPX* and both the genes together in *Arabidopsis*. In transgenics, major alterations were observed at anatomical and molecular level, which benefitted plants to cope with the salt stress. Our findings provide major clues in understanding the regulation of H₂O₂ mediated secondary cell wall synthesis during salt stress. Interestingly, the system-wide effects were different in *PaSOD*, *RaAPX* and dual transgenic lines, indicating a unique response of these lines under control and stress conditions.

Transgenic *Arabidopsis* have higher SOD and APX activity and improved salt tolerance

SOD and APX constitute first line of defense against ROS (Ruth et al. 2002), thus playing an important role in protecting cells against superoxide radicals. The enzyme kinetic analysis showed that the SOD and APX activities were higher in transgenic lines as compared to WT under salt stress (Fig. 1a, b), which indicates efficient scavenging of ROS molecules in transgenic lines. Previous studies showed that higher activities of antioxidant enzymes enhanced plant tolerance to various abiotic stresses (Tang et al. 2006). In our study, WT plants induced the defensive system to protect against free radicals but longer the stress time, the more ROS molecules were produced which impaired antioxidant enzyme activity and as a result ROS could not be efficiently removed. The overexpression of both *PaSOD* and *RaAPX* in 18O line provides capacity to scavenge ROS more efficiently than in either of single transgenic lines (S26 or APX).

The accumulation of proline and soluble sugars has been shown to provide tolerance against osmotic stress in plants (Koster and Lynch 1992). Higher tolerance of transgenic lines to salt stress was thus achieved by accumulating more proline and total soluble sugars as compared to WT. Transgenic plants also exhibit less membrane damage and

change in RWC as compared to WT under salt stress. This was due to the efficient scavenging of ROS in transgenic lines leading to less damage to macromolecules and membrane damage providing salt stress tolerance. Transgenic lines also had improved seed yield and other growth attributes as compared to WT under salt stress.

H₂O₂ as regulator of antioxidant and lignin biosynthesis pathways

The H₂O₂ has been recognized as a signalling molecule at low concentration (Gechev and Hille 2005). It also plays important role during cell wall development (Potikha et al. 1999). The presence of H₂O₂ in the cell wall has been demonstrated with histochemical staining (Olson and Varner 1993), but the mechanism of its generation and regulation is largely unknown. In present study, H₂O₂ levels in all the lines under control and stress conditions were estimated, where H₂O₂ was found to be present at higher concentration in S26 line followed by 18O and APX20 (Fig. 1g, h). The involvement of CuZn-SOD in the supply of H₂O₂ for cell wall lignification was first demonstrated in spinach hypocotyls (Ogawa et al. 1996). In transgenic lines (S26 and 18O), phloroglucinol reaction showed enhanced lignification in the xylem (Fig. 3), that corresponds to the sites of distribution of CuZn-SOD and generation of H₂O₂ (Ogawa et al. 1997). A novel isoform of CuZn-SOD in Scot pine localized in sieve elements, and secondary cell wall of the xylem was found to be the regulator of H₂O₂ production (Karpinska et al. 2001). Thus, it appears that the H₂O₂ produced by SOD acts as signalling molecule inducing cascade of events which finally turn on the secondary cell wall biosynthesis genes (Fig. 5). In comparison to WT, the accumulation of H₂O₂ paralleled the increase in lignin content in SOD overexpressing lines (Fig. 1g). A positive correlation ($r > 0.6$) between H₂O₂ and lignin content was observed under salt stress. This result suggests that the H₂O₂ content in transgenic lines S26 and 18O is closely associated with the lignin accumulation. The 100 mM salt stress was found to be optimum stress level which boosts the H₂O₂ levels that directly affects the lignin content. Enrichment analysis also revealed that H₂O₂ metabolic and biosynthetic processes were highly enriched in 18O transgenic line at 100 mM NaCl (Supplementary Figures S12, S13).

Lignification of vascular bundles improved salt stress tolerance

Several studies have shown increase in lignin content or change in its composition under stress conditions (Gill et al. 2010b; Moura et al. 2010). The presence of extra copy of *PaSOD* helps in efficient scavenging of superoxide

molecules along with lignification of the vascular system leading to improved salt stress tolerance of transgenic plant. This was evident from the observation that xylem cells in 18O transgenics were thick and large (Table 1) due to heavy lignin deposition followed by S26 line (Fig. 2). Phloroglucinol-HCl and Mäule staining are considered to stain specifically cinnamaldehyde end groups (Adler et al. 1948) and syringyl (S) units in lignin (Lewis and Yamamoto 1990), respectively. Intense lignin staining was observed in xylem cells and fibers (Figs. 3, 4). This indicates that lignin is specifically and heavily deposited in xylem cells and fibers of 18O stems under salt stress. In addition, ecotopic secondary cell wall thickening was also observed in the cortex and epidermis of 18O line under 100 mM NaCl. Previous studies have shown that ecotopic deposition of lignin is regulated by overexpression of NAC and MYB transcription factors (Kubo et al. 2005; Mitsuda et al. 2005, 2007; Zhong et al. 2006, 2008; Zhong and Ye 2007; Zhou et al. 2009). Moreover, the transgenic plants had an altered monolignol composition with an increased S:G ratio (Table 2). A study on peroxidase activity showed that the increase in the S/G ratio, could be partly attributed to the increased activity of a syringaldazine peroxidase linked to the enhanced cell wall biosynthesis (Aoyama et al. 2001).

Perturbations in phenylpropanoid pathway relates to enhanced salt tolerance of SOD overexpressing lines

RNA-seq analysis revealed that in S26 and 18O lines, most of the genes involved in lignin biosynthesis were upregulated during salt stress (Fig. 6a, b), where a shift in expression pattern was observed from control to salt stress condition and major upregulation in lignin biosynthesis genes was observed in 18O followed by S26 (Fig. 6b). CuZn-SOD is essential to lignification since it supplies H₂O₂ and protects the peroxidase from inactivation by superoxide as reported by Ogawa et al. (1997). The involvement of SOD and H₂O₂ in cell wall lignification was further supported by several groups independently (Karpinska et al. 2001; Kim and Barbara 2008). It was also shown that H₂O₂ signalling mediates upregulation of lignin biosynthesis genes indirectly through MAP kinases and NAC, MYB and WRKY TF's (Fujita et al. 2006). Several TFs regulating secondary cell wall deposition have been identified in previous studies (Zhong and Ye 2007), but little is known about the signalling cascade regulating salt stress-induced secondary cell wall synthesis. It is presumed that increased H₂O₂ levels could be perceived directly by TFs that orchestrate downstream cascade (Miller et al. 2008). It is found that stress leads to the production of H₂O₂ which serves as a secondary messenger and relay the signal to MAP-kinases (MEKK1, MPK3, MPK4 and MPK6) and TFs, such as

NAC, ZAT, WRKY, DREB, bZIP and MYB (Zhong et al. 2008). In RNA-seq study, C3H, NAC, MYB and WRKY TFs were found to be among the top 10 TFs which were upregulated at 100 mM salt stress conditions in 18O lines. This observation suggests that the signalling cascade of secondary cell wall synthesis is activated under salt stress in 18O line.

Deletion analyses in the promoters of PAL and 4CL genes identified cis-acting (AC) elements critical for their expression in vascular tissues (Hauffe et al. 1991; Levya et al. 1992). It was shown that MYB protein was able to bind to the AC elements and turn on the expression of a reporter gene driven by the PAL and 4CL1 promoter (Zhou et al. 2009). In RNA-seq analysis, MYB58, MYB61 and MYB63 were found to be upregulated in both S26 and 18O lines at 100 mM NaCl. These MYBs are part of SND1/NST1 mediated transcription network involved in regulation of secondary cell wall biosynthesis in fibers and vessels, where they bind to the AC elements in the promoters and serve as common means for the coordinated regulation of genes in the entire monolignol biosynthesis pathway (Zhong et al. 2008; Zhou et al. 2009). Three NAC TFs, NST1, NST2 and NST3 were also shown to regulate the entire secondary cell wall program in *Arabidopsis* (Zhong et al. 2008). The SND1 and NST1 (SND3) act as master switches activating downstream targets, MYB46 and MYB83 which are positive regulators of lignin biosynthesis in fibers and vessels (Zhong and Ye 2007). Most of these TFs were upregulated in S26 and 18O lines (Fig. 5b). The NST homologs VND6 and VND7, which are involved in xylem vessel formation, were able to upregulate MYB46 directly, suggesting that they also regulate the lignin pathway (Mitsuda et al. 2007). H₂O₂ also acts as a potent activator of a MAPK cascades in various tissues (Desikan et al. 1999). Constitutive activation of a H₂O₂ responsive MAPK was shown to mediate cross-tolerance to various environmental stresses by activating stress-responsive genes (Kovtun et al. 2000). We found that ANP1, ANP2, NDPK2, MAPK3, MAPK6 and MEKK4 kinases were highly upregulated in 18O transgenic line which in turn activates the members of C3H TF family. Enrichment analysis with AgriGo, also showed that protein serine/threonine kinase activity (among catalytic activity) and MAPKKK cascade (among molecular processes), which are involved in downstream signalling were highly enriched in 18O under 100 mM NaCl (Supplementary Figures 11, 12).

In conclusion, we suggest that H₂O₂ mediates the signalling in transgenics overexpressing SOD and APX genes leading to heavy deposition of lignin in vascular system and interfascicular cambium. The enhanced lignification along with accumulation of osmoprotectants (proline and soluble sugars) are important processes that increase salt stress tolerance in the transgenic plants.

Availability of supporting data

The transcriptome sequence data reported in this study has been submitted as BioProject ID PRJNA217812 to the NCBI Sequence Read Archive under accession number SRP029598. All the supporting data are included as additional files.

Acknowledgments This work was supported by Grants from the Council of Scientific and Industrial Research (CSIR), New Delhi, India under CSIR Network Projects: SIMPLE (BSC0109) and Plagen (BSC0107) and Indo-German Science and Technology Centre (IGSTC), India. A.S. and T.G. acknowledge fellowships awarded by the CSIR, India. Mr. Sanjoy Chanda is acknowledged for technical help in confocal microscopy. We thank Dr. Ivelin Pantchev, Associate Professor, Sofia University, Sofia, Bulgaria for critically reading the manuscript. This paper represents CSIR-IHBT communication number 3567.

References

- Adler E, Bjorkquist KJ, Haggroth S (1948) Über die Ursache der Farbreaktionen des Holzes. Acta Chem Scand 2:93–94
- Akin DE, Morrison WH, Himmelsbach DS (1993) Characterization of digestion residues of alfalfa and orchardgrass leaves by microscopic, spectroscopic and chemical analysis. J Sci Food Agric 63:339–347
- Almagro L, Ros LVG, Bekchi-Navarro S, Bru R, Barcelo AR, Paredo MA (2009) Class III peroxidases in plant defence reactions. J Exp Bot 60:377–390
- Altschul SF, Gish W, Miller W, Myers EW, Lipman DJ (1990) Basic local alignment search tool. J Mol Biol 215:403–410
- Aoyama W, Matsumura A, Tsutsumi Y, Nishida T (2001) Lignification and peroxidase in tension wood of *Eucalyptus viminalis* seedlings. J Wood Sci 47:419–424
- Asada K (1999) The water–water cycle in chloroplasts: scavenging of active oxygen and dissipation of excess photons. Annu Rev Plant Physiol Plant Mol Biol 50:601–639
- Barrs HD, Weatherley PE (1962) A re-examination of the relative turgidity technique for estimating water deficits in leaves. Aust J Biol Sci 15:413–428
- Bates L, Waldren R, Teare ID (1973) Rapid determination of free proline for water–stress studies. Plant Soil 39:205–207
- Bradford MM (1976) A rapid and sensitive method for the quantitation of microgram quantities of protein utilizing the principle of protein–dye binding. Anal Biochem 72:248–254
- Czechowski T, Stitt M, Altman T, Udvardi MK, Scheible WR (2005) Genome-wide identification and testing of superior reference genes for transcript normalization in *Arabidopsis*. Plant Physiol 139:5–17
- Desikan R, Clarke A, Hancock JT, Neill SJ (1999) H₂O₂ activates a MAP kinase-like enzyme in *Arabidopsis thaliana* suspension cultures. J Exp Bot 50:1863–1866
- Fujita M, Fujita Y, Noutoshi Y, Takahashi F, Narusaka Y, Yamaguchi-Shinozaki K, Shinozaki K (2006) Crosstalk between abiotic and biotic stress responses: a current view from the points of convergence in the stress signalling networks. Curr Opin Plant Biol 9:436–442
- Gahlan P, Singh HR, Shankar R, Sharma N, Kumari A, Chawla V, Ahuja PS, Kumar S (2012) De novo sequencing and characterization of *Picrorhiza kurroa* transcriptome at two temperatures showed major transcriptome adjustments. BMC Genom 13:126

- Gechev TS, Hille J (2005) Hydrogen peroxide as a signal controlling plant programmed cell death. *J Cell Biol* 168:17–20
- Ghawana S, Paul A, Kumar H, Kumar A, Singh H, Bhardwaj PK, Rani A, Singh RS, Raizada J, Singh K, Kumar S (2007) An RNA isolation system for plant tissues rich in secondary metabolites. *BMC Res Notes* 4:85
- Gill T, Kumar S, Ahuja PS, Sreenivasulu Y (2010a) Over-expression of *Potentilla* superoxide dismutase improves salt stress tolerance during germination and growth in *Arabidopsis thaliana*. *J Plant Genet Transgenics* 1:1–10
- Gill T, Sreenivasulu Y, Kumar S, Ahuja PS (2010b) Over-expression of superoxide dismutase exhibits lignification of vascular structures in *Arabidopsis thaliana*. *J Plant Physiol* 167:757–760
- Hauffe KD, Paszkowski U, Schulze-Lefert P, Hahlbrock K, Dangl JL, Douglas CJ (1991) A parsley 4CL-1 promoter fragment specifies complex expression patterns in transgenic tobacco. *Plant Cell* 3:435–443
- Hilal M, Zenoff AM, Ponessa G, Moreno H, Massa ED (1998) Saline stress alters the temporal patterns of xylem differentiation and alternative oxidase expression in developing soybean roots. *Plant Physiol* 117:695–701
- Irigoyen JJ, Emerich DW, Sanchez-Diaz M (1992) Water stress induced changes in concentrations of proline and total soluble sugars in nodulated alfalfa (*Medicago sativa*) plants. *Physiol Plant* 84:55–60
- Jbir N, Chaïbi W, Ammar S, Jemmali A, Ayadi A (2001) Root growth and lignification of two wheat species differing in their sensitivity to NaCl, in response to salt stress. *Compt Rendus Acad Sci III Sci Vie* 324:863–868
- Karahara I, Ikeda A, Kondo T, Uetake Y (2004) Development of the Casparian strip in primary roots of maize under salt stress. *Planta* 219:41–47
- Karpinska B, Karlsson M, Schinkel H, Steller S, Suss KH, Melzer M, Wingsle G (2001) A novel superoxide dismutase with a high isoelectric point in higher plants: expression, regulation and protein localisation. *Plant Physiol* 126:1668–1677
- Kim HJ, Barbara T (2008) Involvement of extracellular Cu/Zn superoxide dismutase in cotton fiber primary and secondary cell wall biosynthesis. *Plant Signal Behav* 3:1119–1121
- Kirk TK, Obst JR (1988) Lignin Determination. In: Wood WA, Kellogg ST (eds) *Methods in enzymology*, volume 161, biomass, Part B: lignin, pectin, and chitin. Academic Press Inc, New York, pp 87–101
- Koster KL, Lynch DV (1992) Solute accumulation and compartmentation during the cold acclimation of puma rye. *Plant Physiol* 98:108–113
- Kovtun Y, Chiu WL, Tena G, Sheen J (2000) Functional analysis of oxidative stress-activated mitogen-activated protein kinase cascade in plants. *Proc Natl Acad Sci USA* 97:2940–2945
- Kubo M, Udagawa M, Nishikubo N, Horiguchi G, Yamaguchi M, Ito J, Mimura T, Fukuda H, Demura T (2005) Transcription switches for protoxylem and metaxylem vessel formation. *Genes Dev* 19:1855–1860
- Kumar S, Sahoo R, Ahuja PS (2002) Isozyme of autoclavable superoxide dismutase (SOD), a process for the identification and extraction of the SOD in cosmetic, food and pharmaceutical compositions. US Patent No. 6,485,950 B1
- Levy A, Liang X, Pintor-Toro JA, Dixon RA, Lamb CJ (1992) cis-Element combinations determine phenylalanine ammonia-lyase gene tissue-specific expression patterns. *Plant Cell* 4:263–271
- Lewis NG, Yamamoto E (1990) Lignin: occurrence, biogenesis, and biodegradation. *Annu Rev Plant Physiol Plant Mol Biol* 41:455–496
- Liyama K, Wallis PJ (1990) Determination of lignins in herbaceous plants by improved acetylbromide procedure. *J Sci Food Agric* 51:145–161
- Lutts S, Kinet JM, Bouharmont J (1996) NaCl-induced senescence in leaves of rice (*Oryza sativa* L.) cultivars differing in salinity resistance. *Ann Bot* 78:389–398
- Miller G, Shulaev V, Mittler R (2008) Reactive oxygen signalling and abiotic stress. *Physiol Plantarum* 133:481–489
- Miller G, Suzuki N, Ciftci-Yilmaz S, Mittler R (2010) Reactive oxygen species homeostasis and signalling during drought and salinity stresses. *Plant Cell Environ* 33:453–467
- Mitsuda N, Seki M, Shinozaki K, Ohme-Takagi M (2005) The NAC transcription factors NST1 and NST2 of *Arabidopsis* regulate secondary wall thickenings and are required for anther dehiscence. *Plant Cell* 17:2993–3006
- Mitsuda N, Iwase A, Yamamoto H, Yoshida M, Seki M, Shinozaki K, Ohme-Takagi M (2007) NAC transcription factors, NST1 and NST3, are key regulators of the formation of secondary walls in woody tissues of *Arabidopsis*. *Plant Cell* 19:270–280
- Moura JCMS, Bonine CAV, Viana JOF, Dornelas MC, Mazzafera P (2010) Abiotic and biotic stresses and changes in the lignin content and composition in plants. *J Integr Plant Biol* 52:360–376
- Murashige T, Skoog F (1962) A revised medium for rapid growth and bioassays with tobacco tissue cultures. *Physiol Plantarum* 15:473–497
- Nakano Y, Asada K (1981) Hydrogen peroxide is scavenged by ascorbate-specific peroxidase in spinach chloroplasts. *Plant Cell Physiol* 22:867–880
- Neill SJ, Desikan R, Hancock J (2002) Hydrogen peroxide signalling. *Curr Opin Plant Biol* 5:388–395
- Ogawa K, Kanematsu S, Asada K (1996) Intra- and extra-cellular localization of “cytosolic” CuZn-superoxide dismutase in spinach leaf and hypocotyl. *Plant Cell Physiol* 37:790–799
- Ogawa K, Kanematsu S, Asada K (1997) Generation of superoxide anion and localization of CuZn-superoxide dismutase in the vascular tissue of spinach hypocotyls: their association with lignification. *Plant Cell Physiol* 38:1118–1126
- Olson PD, Varner JE (1993) Hydrogen peroxide and lignification. *Plant J* 4:887–892
- Pfaffl MW, Horgan GW, Dempfle L (2002) Relative expression software tool (REST) for group-wise comparison and statistical analysis of relative expression results in real-time PCR. *Nucleic Acids Res* 30:36
- Potikha TS, Collins CC, Johnson DI, Delmer DP, Levine A (1999) The involvement of hydrogen peroxide in the differentiation of secondary walls in cotton fibers. *Plant Physiol* 119:849–858
- Quiroga M, Guerrero C, Botella MA, Barcelo A, Amaya I, Medina MI, Alonso FJ, de Forchetti SM, Tigier H, Valpuesta V (2000) A tomato peroxidase involved in the synthesis of lignin and suberin. *Plant Physiol* 122:1119–1127
- Ros-Barceló A (1995) Peroxidase and not laccase is the enzyme responsible for cell wall lignification in the secondary thickening of xylem vessels in *Lupinus*. *Protoplasma* 186:41–44
- Rozen S, Skaletsky H (2000) Primer3 on the WWW for general users and for biologist programmers. *Methods Mol Biol* 132:365–386
- Ruth GA, Neval E, Lenwood SH (2002) Role of superoxide dismutases (SODs) in controlling oxidative stress in plants. *J Exp Bot* 372:1331–1341
- Sambrook J, Russell DW (2001) *Molecular cloning: a laboratory manual*, 3rd edn. Cold Spring Harbor laboratory Press, New York
- Sánchez-Aguayo I, Rodríguez-Galán JM, García R, Torreblanca J, Pardo JM (2004) Salt stress enhances xylem development and expression of S-adenosyl-L-methionine synthase in lignifying tissues of tomato plants. *Planta* 220:278–285
- Schmid R, Blaxter ML (2008) annot8r: GO, EC and KEGG annotation of EST datasets. *BMC Bioinformatics* 9:180
- Sonja V, Noctor G, Foyer CH (2002) Are leaf hydrogen peroxide concentrations commonly overestimated? The potential influence of

- artefactual interference by tissue phenolics and ascorbate. *Plant Physiol Biochem* 40:501–507
- Tang L, Kwon SY, Kim SY, Kim JS, Choi JS, Kwang YC, Sung CK, Kwak SS, Lee HS (2006) Enhanced tolerance of transgenic potato plants expressing both superoxide dismutase and ascorbate peroxidase in chloroplasts against oxidative stress and high temperature. *Plant Cell Rep* 25:1380–1386
- Trapnell C, Roberts A, Goff L, Pertea G, Kim D, Kelley DR, Pimentel H, Salzberg SL, Rinn JL, Pachter L (2012) Differential gene and transcript expression analysis of RNA-seq experiments with TopHat and Cufflinks. *Nat Protoc* 7:562–578
- Vierling E, Kimpel JA (1992) Plant responses to environmental stress. *Curr Opin Biotechnol* 3:164–170
- Zhong R, Ye ZH (2007) Regulation of cell wall biosynthesis. *Curr Opin Plant Biol* 10:564–572
- Zhong R, Demura T, Ye ZH (2006) SND1, a NAC domain transcription factor, is a key regulator of secondary wall synthesis in fibers of *Arabidopsis*. *Plant Cell* 18:3158–3170
- Zhong R, Lee C, Zhou J, McCarthy RL, Ye ZH (2008) A battery of transcription factors involved in the regulation of secondary cell wall biosynthesis in *Arabidopsis*. *Plant Cell* 20:2763–2782
- Zhou J, Lee C, Zhong R, Ye ZH (2009) MYB58 and MYB63 are transcriptional activators of the lignin biosynthetic pathway during secondary cell wall formation in *Arabidopsis*. *Plant cell* 121:248–266
- Zhu JK (2002) Salt and drought stress signal transduction in plants. *Annu Rev Plant Biol* 53:247–273